

Study of $J/\psi \rightarrow \omega K^+ K^-$

M. Ablikim¹, J. Z. Bai¹, Y. Ban¹⁰, J. G. Bian¹, D. V. Bugg¹⁹, X. Cai¹,
 J. F. Chang¹, H. F. Chen¹⁶, H. S. Chen¹, H. X. Chen¹, J. C. Chen¹, Jin Chen¹,
 Jun Chen⁶, M. L. Chen¹, Y. B. Chen¹, S. P. Chi², Y. P. Chu¹, X. Z. Cui¹,
 H. L. Dai¹, Y. S. Dai¹⁸, Z. Y. Deng¹, L. Y. Dong¹, S. X. Du¹, Z. Z. Du¹, J. Fang¹,
 S. S. Fang², C. D. Fu¹, H. Y. Fu¹, C. S. Gao¹, Y. N. Gao¹⁴, M. Y. Gong¹,
 W. X. Gong¹, S. D. Gu¹, Y. N. Guo¹, Y. Q. Guo¹, Z. J. Guo¹⁵, F. A. Harris¹⁵,
 K. L. He¹, M. He¹¹, X. He¹, Y. K. Heng¹, H. M. Hu¹, T. Hu¹, G. S. Huang^{1†},
 L. Huang⁶, X. P. Huang¹, X. B. Ji¹, Q. Y. Jia¹⁰, C. H. Jiang¹, X. S. Jiang¹,
 D. P. Jin¹, S. Jin¹, Y. Jin¹, Y. F. Lai¹, F. Li¹, G. Li¹, H. H. Li¹, J. Li¹, J. C. Li¹,
 Q. J. Li¹, R. B. Li¹, R. Y. Li¹, S. M. Li¹, W. G. Li¹, X. L. Li⁷, X. Q. Li⁹,
 X. S. Li¹⁴, Y. F. Liang¹³, H. B. Liao⁵, C. X. Liu¹, F. Liu⁵, Fang Liu¹⁶, H. M. Liu¹,
 J. B. Liu¹, J. P. Liu¹⁷, R. G. Liu¹, Z. A. Liu¹, Z. X. Liu¹, F. Lu¹, G. R. Lu⁴,
 J. G. Lu¹, C. L. Luo⁸, X. L. Luo¹, F. C. Ma⁷, J. M. Ma¹, L. L. Ma¹¹, Q. M. Ma¹,
 X. Y. Ma¹, Z. P. Mao¹, X. H. Mo¹, J. Nie¹, Z. D. Nie¹, S. L. Olsen¹⁵,
 H. P. Peng¹⁶, N. D. Qi¹, C. D. Qian¹², H. Qin⁸, T. N. Ruan¹⁶, J. F. Qiu¹,
 Z. Y. Ren¹, G. Rong¹, L. Y. Shan¹, L. Shang¹, D. L. Shen¹, X. Y. Shen¹,
 H. Y. Sheng¹, F. Shi¹, X. Shi¹⁰, H. S. Sun¹, S. S. Sun¹⁶, Y. Z. Sun¹, Z. J. Sun¹,
 X. Tang¹, N. Tao¹⁶, Y. R. Tian¹⁴, G. L. Tong¹, G. S. Varner¹⁵, D. Y. Wang¹,
 J. Z. Wang¹, K. Wang¹⁶, L. Wang¹, L. S. Wang¹, M. Wang¹, P. Wang¹,
 P. L. Wang¹, S. Z. Wang¹, W. F. Wang¹, Y. F. Wang¹, Zhe Wang¹, Z. Wang¹,
 Zheng Wang¹, Z. Y. Wang¹, C. L. Wei¹, D. H. Wei³, N. Wu¹, Y. M. Wu¹,
 X. M. Xia¹, X. X. Xie¹, B. Xin⁷, G. F. Xu¹, H. Xu¹, Y. Xu¹, S. T. Xue¹,
 M. L. Yan¹⁶, F. Yang⁹, H. X. Yang¹, J. Yang¹⁶, S. D. Yang¹, Y. X. Yang³, M. Ye¹,
 M. H. Ye², Y. X. Ye¹⁶, L. H. Yi⁶, Z. Y. Yi¹, C. S. Yu¹, G. W. Yu¹, C. Z. Yuan¹,
 J. M. Yuan¹, Y. Yuan¹, Q. Yue¹, S. L. Zang¹, Yu. Zeng¹, Y. Zeng⁶, B. X. Zhang¹,
 B. Y. Zhang¹, C. C. Zhang¹, D. H. Zhang¹, H. Y. Zhang¹, J. Zhang¹,
 J. Y. Zhang¹, J. W. Zhang¹, L. S. Zhang¹, Q. J. Zhang¹, S. Q. Zhang¹,
 X. M. Zhang¹, X. Y. Zhang¹¹, Y. J. Zhang¹⁰, Y. Y. Zhang¹, Yiyun Zhang¹³,
 Z. P. Zhang¹⁶, Z. Q. Zhang⁴, D. X. Zhao¹, J. B. Zhao¹, J. W. Zhao¹, M. G. Zhao⁹,
 P. P. Zhao¹, W. R. Zhao¹, X. J. Zhao¹, Y. B. Zhao¹, Z. G. Zhao^{1*}, H. Q. Zheng¹⁰,
 J. P. Zheng¹, L. S. Zheng¹, Z. P. Zheng¹, X. C. Zhong¹, B. Q. Zhou¹,
 G. M. Zhou¹, L. Zhou¹, N. F. Zhou¹, K. J. Zhu¹, Q. M. Zhu¹, Y. C. Zhu¹,
 Y. S. Zhu¹, Yingchun Zhu¹, Z. A. Zhu¹, B. A. Zhuang¹, B. S. Zou¹.

(BES Collaboration)

¹ Institute of High Energy Physics, Beijing 100039, People's Republic of China

² China Center for Advanced Science and Technology (CCAST), Beijing 100080,
 People's Republic of China

³ Guangxi Normal University, Guilin 541004, People's Republic of China

⁴ Henan Normal University, Xinxiang 453002, People's Republic of China

⁵ Huazhong Normal University, Wuhan 430079, People's Republic of China

⁶ Hunan University, Changsha 410082, People's Republic of China

⁷ Liaoning University, Shenyang 110036, People's Republic of China

- ⁸ Nanjing Normal University, Nanjing 210097, People's Republic of China
⁹ Nankai University, Tianjin 300071, People's Republic of China
¹⁰ Peking University, Beijing 100871, People's Republic of China
¹¹ Shandong University, Jinan 250100, People's Republic of China
¹² Shanghai Jiaotong University, Shanghai 200030, People's Republic of China
¹³ Sichuan University, Chengdu 610064, People's Republic of China
¹⁴ Tsinghua University, Beijing 100084, People's Republic of China
¹⁵ University of Hawaii, Honolulu, Hawaii 96822, USA
¹⁶ University of Science and Technology of China, Hefei 230026, People's Republic of China
¹⁷ Wuhan University, Wuhan 430072, People's Republic of China
¹⁸ Zhejiang University, Hangzhou 310028, People's Republic of China
¹⁹ Queen Mary, University of London, London E1 4NS, UK

* Current address: University of Michigan, Ann Arbor, Michigan, 48109, USA

† Current address: Purdue University, West Lafayette, Indiana 47907, USA.

Abstract

New data are presented on $J/\psi \rightarrow \omega K^+ K^-$ from a sample of 58M J/ψ events in the upgraded BES II detector at the BEPC. There is a conspicuous signal for $f_0(1710) \rightarrow K^+ K^-$ and a peak at higher mass which may be fitted with $f_2(2150) \rightarrow K \bar{K}$. From a combined analysis with $\omega \pi^+ \pi^-$ data, the branching ratio $BR(f_0(1710) \rightarrow \pi \pi) / BR(f_0(1710) \rightarrow K \bar{K})$ is < 0.11 at the 95% confidence level.

PACS: 13.25.Gv, 14.40.Gx, 13.40.Hq

In a recent publication, we have presented new data on $J/\psi \rightarrow \omega\pi^+\pi^-$ [1] from a sample of 58M J/ψ events taken in the Beijing Spectrometer (BES) detector at the Beijing Electron Positron Collider. Here we report data on $J/\psi \rightarrow \omega K^+K^-$. Earlier data on this channel with lower statistics have been published by Mark I [2], DM2 [3] and Mark III [4].

The BES II detector is a large solid-angle magnetic spectrometer that is described in detail in Ref. [5]. Charged particles are measured in a vertex chamber and Main Drift Chamber (MDC); these are surrounded by a solenoidal magnet providing a nearly uniform field of 0.4T. Photons are detected in a Barrel Shower Counter (BSC) made of gas proportional tubes interleaved with 12 radiation lengths of lead sheets. A time-of-flight (TOF) hodoscope immediately outside the MDC provides separation between pions, kaons, and protons. The time resolution of the TOF measurement is 180 ps. Further separation is obtained using dE/dx in the MDC.

The point of closest approach of a charged track to the beam is required to be within 2 cm of the beam axis and within 20 cm of the centre of the interaction region along the beam axis. Both photons are required to be isolated from charged tracks by demanding an angle $> 8^\circ$ to the nearest charged track. Any photon with an energy deposit < 30 MeV in the shower counter is rejected. All particles are required to lie well within the acceptance of the detector, with charged tracks having laboratory polar angles θ satisfying $|\cos\theta| < 0.84$ and with transverse momenta > 60 MeV/c.

The ω is observed decaying to $\pi^+\pi^-\pi^0$, so events are selected initially by demanding two photons and four charged tracks with total charge zero. If there are more than two photons, all are tried; an extra photon can arise from interactions of charged particles in the detector. Kaons can be identified up to momenta of 800 MeV/c by TOF and dE/dx measurements. The two slowest particles always have energies < 800 MeV. The first step is to identify one kaon and one pion using TOF and dE/dx . The other two tracks often have momenta too high to be identified by TOF and dE/dx , so a four-constraint kinematic fit is made for the $K^+K^-\pi^+\pi^-\gamma\gamma$ hypothesis. The kinematic fit requires $\chi^2(K^+K^-\pi^+\pi^-\gamma\gamma) < 40$.

The π^0 is selected by requiring $|M_{\gamma\gamma} - M_{\pi^0}| < 0.020$ GeV/c²; the π^0 mass resolution is ~ 15 MeV/c². The resulting $\pi^+\pi^-\pi^0$ mass distribution is shown in Fig. 1. The ω signal is then selected requiring $|M_{\pi^+\pi^-\pi^0} - M_\omega| \leq 40$ MeV/c². The background is fitted by a second order polynomial in $M(\pi^+\pi^-\pi^0)$. A background of $(22.9 \pm 2.0)\%$ is estimated from ω sidebands, defined by $80 \leq |M_{\pi^+\pi^-\pi^0} - M_\omega| \leq 160$ MeV/c²; the error allows for small variations when the location and width of the sidebins are changed.

For a given ω momentum, the mass of the accompanying $K\bar{K}$ pair is unique.

The decay angles of $\pi\pi$ and $K\bar{K}$ in the lab frame are very different except near 0 or 180°. There, the backward π or K differ strongly in momentum and are easily distinguished by momentum, TOF, and dE/dx . As a result, there is a clean separation between $\omega\pi^+\pi^-$ and ωK^+K^- .

Most background originates from $K^+K^-\pi^+\pi^-\pi^0$. The other sources of background are K_S^0 in final states $K_S^0K^\pm\pi^\mp\pi^0$ and $K_S^0K^\pm\pi^\mp\gamma$. Most K_S events are rejected as follows. If $\chi^2(K_S^0K^\pm\pi^\mp\gamma\gamma) < \chi^2(K^+K^-\pi^+\pi^-\gamma\gamma)$ or $\chi^2(K_S^0K^\pm\pi^\mp\gamma) < \chi^2(K^+K^-\pi^+\pi^-\gamma\gamma)$, events are discarded if any $K\pi\pi\pi$ combination has $M(\pi^+\pi^-)$ in the interval 497 ± 25 MeV/ c^2 and $r_{xy} > 3$ mm; here r_{xy} is the distance from the beam axis to the $\pi^+\pi^-$ vertex. This avoids rejecting too many signal events; surviving K_S background is too small to be visible. The beam spot has a σ_x of 0.6 mm, and the resolution of the second vertex is 1.2 mm in xy . After the background subtraction, there are 3438 signal events. From the Monte Carlo simulation, the average detection efficiency is 4.0%.

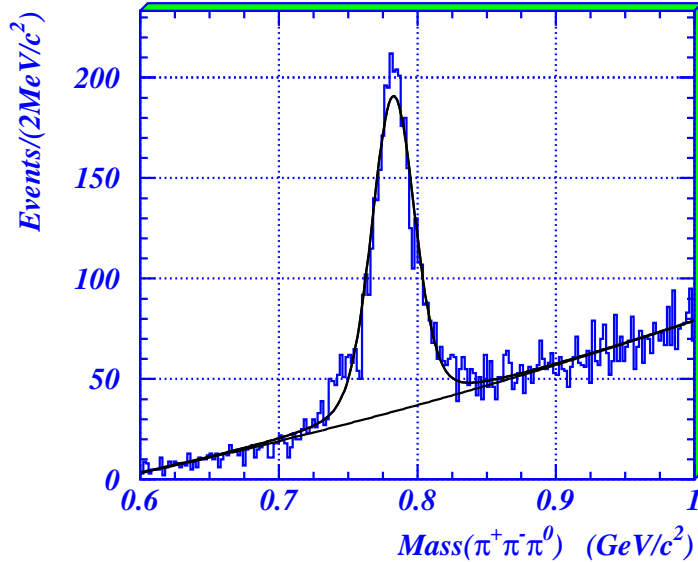


Fig. 1. The ω peak from the selection described in the text; background is estimated from the lower curve.

Fig. 2(a) shows the experimental Dalitz plot, and Figs. 2(c) and (d) show projections on to masses of K^+K^- and ωK ; the shaded area indicates background events from the sideband estimation.

The channels fitted to the data are:

$$\begin{aligned}
 J/\psi &\rightarrow \omega\sigma \\
 &\rightarrow \omega f_0(980) \\
 &\rightarrow \omega f_0(1710) \\
 &\rightarrow \omega f_2(1270)
 \end{aligned}$$

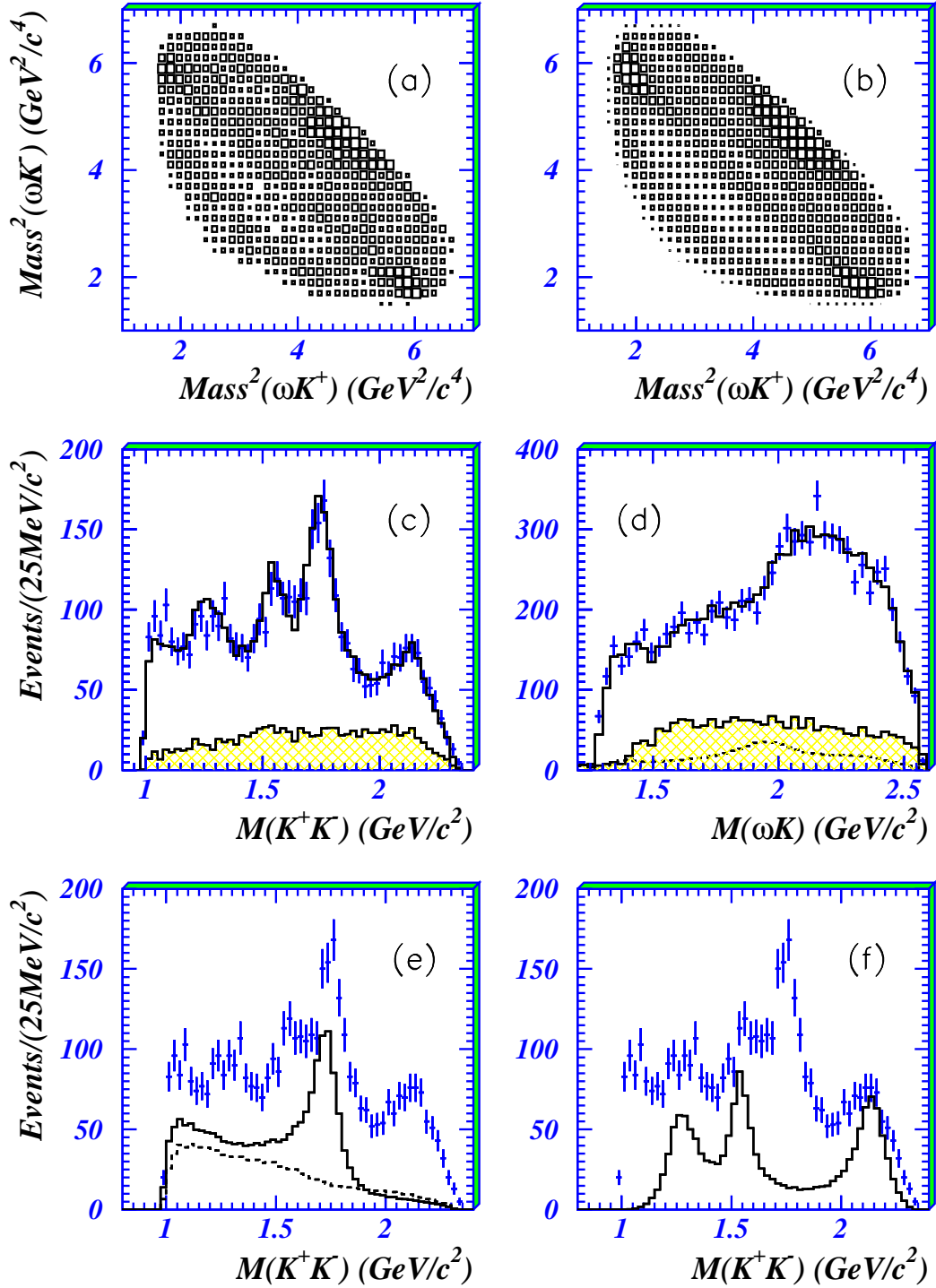


Fig. 2. (a) and (b): Measured and fitted Dalitz plots for $\omega K^+ K^-$; (c) and (d) are projections on to $K^+ K^-$ and ωK mass. In the latter, histograms show the maximum likelihood fit; the shaded region indicates the background estimated from sidebins; the dashed curve in (d) shows the magnitude of the $K_1(1400)$ contribution and a $K\omega$ contribution at 1945 MeV/ c^2 ; (e) and (f) show mass projections of f_0 and f_2 contributions to $K^+ K^-$. The dashed curve of (e) shows the $\sigma \rightarrow K^+ K^-$ S-wave contribution.

$$\begin{aligned}
&\rightarrow \omega f_2'(1525) \text{ or } \omega f_2(1565) \\
&\rightarrow \omega f_2(2150) \\
&\rightarrow K_1(1400)K \\
&\rightarrow K_1(1950)K.
\end{aligned}$$

Amplitudes are fitted to relativistic tensor expressions documented in Ref. [6]. For spin 0 in $K\bar{K}$, two transitions from J/ψ are allowed with orbital angular momenta $\ell = 0$ and 2 in the production process. For spin 2, there are five amplitudes: one with $\ell = 0$, three with $\ell = 2$ and one with $\ell = 4$. In fitting these, Blatt-Weisskopf centrifugal barrier factors are included with a radius of 0.8 fm, though results are insensitive to this choice. In the amplitude analysis, information from the $\omega \rightarrow \pi^+\pi^-\pi^0$ decay is included in the tensor expressions.

The polarisation vector of the ω lies along the normal to its decay plane. The correlation between this polarisation vector, the production plane, and the decay of the f_J to K^+K^- is sensitive to the spin of f_J and also to the helicity amplitudes for its production. This correlation cannot readily be displayed, since it depends on five angles; however, tests with different J^P demonstrate the sensitivity to quantum numbers.

Fig. 2(b) shows the Dalitz plot from the log likelihood fit described below. Histograms on Figs. 2(e) and (f) show projections of f_0 and f_2 contributions to this fit.

The $\omega\pi^+\pi^-$ data of Ref. [1] determine all helicity amplitudes for production of $f_2(1270)$ well. In fitting present data, the relative magnitudes of these amplitudes are fixed to values from $\omega\pi\pi$. Contributions from $f_0(980)$ are likewise fixed from the signal observed in $\omega\pi^+\pi^-$; its branching ratio $K\bar{K}/\pi\pi$ is taken from the Flatté formula fitted to $J/\psi \rightarrow \phi\pi^+\pi^-$ and ϕK^+K^- [7], where there are conspicuous $f_0(980)$ signals. Phases for $f_2(1270)$ and $f_0(980)$ amplitudes are fitted freely, since they arise from multiple scattering, which is different in $K\bar{K}$ and $\pi\pi$ final states.

For other components, there is a general problem in isolating f_0 from possible f_2 for two reasons. Firstly, five 2^+ amplitudes can simulate two 0^+ amplitudes closely; amplitudes with $J^P = 2^+$ may be identified if they give rise to decay angular distributions which are non-isotropic. Secondly, fitted 2^+ amplitudes can fluctuate for angles outside the acceptance. For high K^+K^- mass above 2 GeV/ c^2 , this latter problem is somewhat reduced, because the $\ell = 4$ amplitude is suppressed by the strong centrifugal barrier for production.

We use σ to denote a broad K^+K^- S-wave contribution. We find that it peaks towards the lower $K\bar{K}$ masses as shown by the dashed curve of Fig. 2(e). However, the dependence on mass above 1 GeV is somewhat uncertain. Many alternative fits have been tried with similar results. A component peaking

towards threshold is required; without it, the fit to the $K\bar{K}$ mass distribution of Fig. 2(c) is bad. We have therefore tried parametrisations using the σ pole of Ref. [1], and a coupling constant of the form $G_1 + G_2s$ or $G_1 + G_2/s$. The optimum fit requires a slightly more rapid fall with s than the σ pole, in order to fit four points at the lowest $K\bar{K}$ masses. However, we regard this as unphysical and therefore eventually choose to use the σ pole of Ref. [1] unchanged, with $G_2 = 0$. Note that there is a substantial constructive interference in present data between $f_0(980)$ and σ amplitudes at masses close to threshold.

A dominant feature is $f_0(1710)$; the present data are consistent with earlier studies which identify $J = 0$ [8,9]. They are also consistent with the absence of any significant $J = 2$ contribution. The fitted $f_0(1710)$ optimises at $M = 1738 \pm 30 \text{ MeV}/c^2$, $\Gamma = 125 \pm 20 \text{ MeV}/c^2$. The error in the mass is mostly systematic, and arises from uncertainty in the σ amplitude with which $f_0(1710)$ interferes; the error in Γ is mostly statistical, but includes allowance for interference with the remaining 0^+ amplitude. Earlier BES II data on $J/\psi \rightarrow \gamma K^+ K^-$ and $\gamma K_S^0 K_S^0$ gave $M = 1740 \pm 4(\text{stat})_{-25}^{+10}(\text{syst}) \text{ MeV}/c^2$ and $\Gamma = 166_{-8}^{+5} \text{ }_{-10}^{+15} \text{ MeV}/c^2$ [8].

A fit to the $1738 \text{ MeV}/c^2$ peak with spin 2 uses five amplitudes and gives log likelihood worse than spin 0 by only 15; the fit is shown in Fig. 3. However, the fit with spin 0 uses only two production amplitudes with $\ell = 0$ and 2. The fit with spin 0 requires an $\ell = 0$ amplitude which is completely dominant over $\ell = 2$. However, for spin 2 the $\ell = 2$ amplitudes dominate over $\ell = 0$. The phase space available in the process $J/\psi \rightarrow \omega f_J(1710)$ is rather limited, and the $\ell = 2$ and 4 centrifugal barriers for the production process should suppress those amplitudes strongly. If the $\ell = 2$ and 4 amplitudes are removed, spin 0 gives a fit better than spin 2 by 90 in log likelihood.

This pattern of behaviour is symptomatic of what is required for spin 2 to simulate spin 0. The spin 2 amplitude with $\ell = 0$ has a unique dependence on angles; it contains a distinctive term $3 \cos^2 \alpha_K - 1$, where α_K is the decay angle of the K^+ in the resonance rest frame, with respect to the direction of the recoil ω . Simulation of spin 0 requires large $J = 2$ $\ell = 2$ and 4 amplitudes to produce compensating terms in $\sin^2 \alpha_K$. Although this is suspicious, the $J = 2$ possibility cannot be ruled out from present data.

We discuss next the branching ratio of $f_0(1710)$ between $K\bar{K}$ and $\pi\pi$, using information from $J/\psi \rightarrow \omega\pi^+\pi^-$ [1], where statistics of $\sim 40K$ events are available. In those data, there is no definite evidence for the presence of $f_0(1710)$; if its mass is scanned, there is no optimum around $1710 \text{ MeV}/c^2$, and the fitted $f_0(1710)$ is only $0.43 \pm 0.21\%$ of $\omega\pi^+\pi^-$. In the $\omega K^+ K^-$ data presented here, the $f_0(1710)$ intensity is $(38 \pm 6)\%$ of the data within the same acceptance as for $\omega\pi^+\pi^-$; the error is almost entirely systematic, and

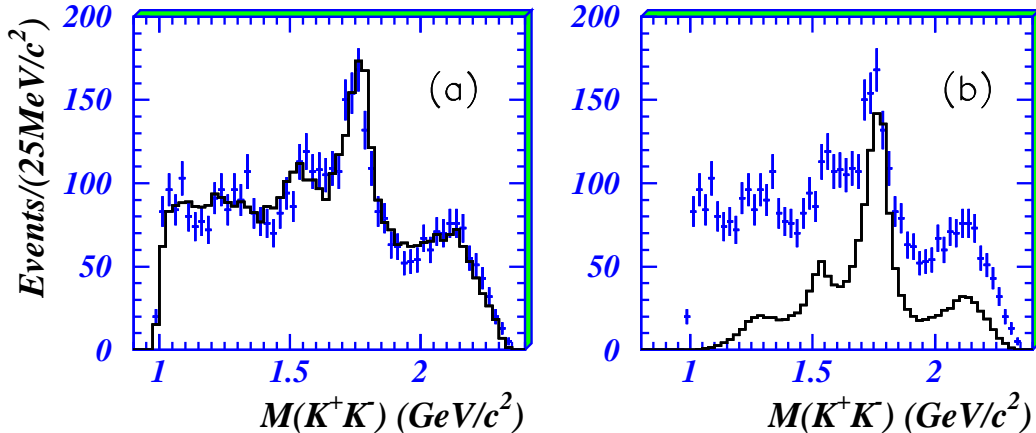


Fig. 3. (a) The projection on to $M(K^+K^-)$ from an alternative fit using $f_2(1710)$, (b) the contribution from $J^P = 2^+$.

covers all alternative parametrisations of the σ amplitude and removing the $K_1(1400)$. The branching fraction for $J/\psi \rightarrow \omega f_0(1710)$, $f_0(1710) \rightarrow K^+K^-$ is $(6.6 \pm 1.3) \times 10^{-4}$. We find at the 95% confidence level

$$\frac{BR(f_0(1710) \rightarrow \pi\pi)}{BR(f_0(1710) \rightarrow K\bar{K})} < 0.11, \quad (1)$$

where all charge states for decay are taken into account.

One caveat is necessary. In our study of $J/\psi \rightarrow \phi\pi^+\pi^-$ and ϕK^+K^- [7], definite evidence is found for an $f_0(1770)$, distinct from $f_0(1710)$ and decaying to $\pi\pi$ (and possibly weakly to $K\bar{K}$). There is a remote possibility that $f_0(1710)$ and $f_0(1770)$ are both present in $\omega\pi\pi$ data but cancel by destructive interference. Such a cancellation would require that they have the same magnitudes but opposite phases. Even then, the cancellation is incomplete, because they have different masses and widths. Allowing for this possible cancellation, the upper limit of the branching ratio given in eqn. (1) could increase to 0.16 if the magnitudes happen to be equal, which is unlikely.

The peak in Fig. 2(c) at ~ 1550 MeV/ c^2 may be fitted with either $f'_2(1525)$ or $f_2(1565)$, or both. Spin 2 is required by non-isotropic decay angular distributions; a fit with an f_0 with the same mass and width gives a worse log likelihood by 64. Also no $f_0(1500)$ is visible in the $\omega\pi^+\pi^-$ data of Ref. [1]. If the peak is fitted with $f'_2(1525)$, the branching fraction is close to that for $f_2(1270) \rightarrow K\bar{K}$. However, because of interferences between helicity amplitudes, the branching fraction could be a factor 2 larger or smaller. If the peak is fitted with $f_2(1565)$, the branching fraction is similar to that of $f_2(1565)$ in $\omega\pi\pi$ data, but again could be a factor 2 larger or smaller. The fit shown in Fig. 2 uses $f'_2(1525)$. The branching ratio of $f_2(1270)$ between $K\bar{K}$ and $\pi\pi$

is $(5.2 \pm 2.5)\%$, consistent with the range of values quoted by the Particle Data Group [9]; again the error arises from flexibility in interferences between helicity amplitudes.

There is a further feature at $\sim 2150 \text{ MeV}/c^2$ in the K^+K^- mass spectrum. Some spin ≥ 2 component is required by non-isotropic decay angular distributions. An optimum fit to present data may be achieved with a mass of $2150 \pm 20 \text{ MeV}/c^2$ and a width $\Gamma = 150 \pm 30 \text{ MeV}/c^2$; these values are within a few MeV/c^2 of PDG values. Errors are mostly statistical but also cover changes when the small amplitudes are omitted from the fit. The data do not rule out the possibility of spin 4, but the fit is consistent with the known $f_2(2150)$ [9].

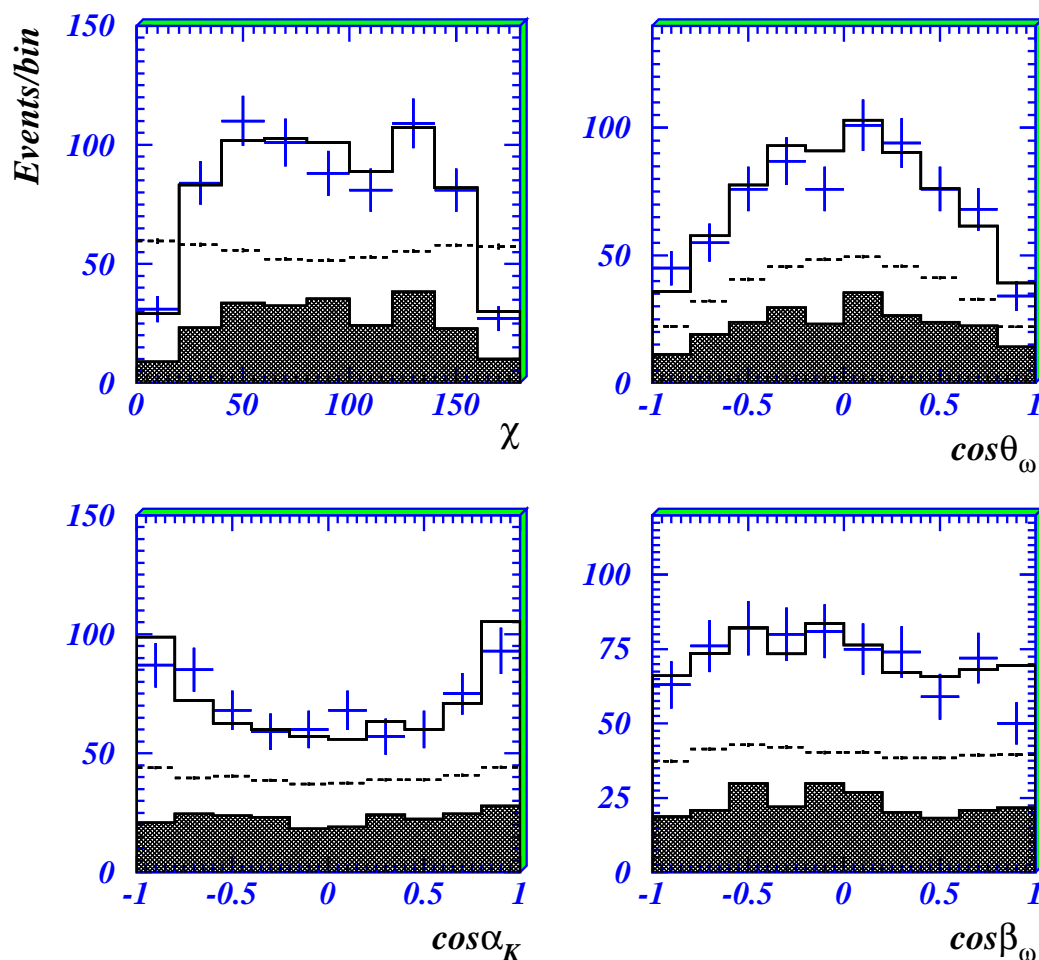


Fig. 4. Angular distributions for $M_{KK} > 2000 \text{ MeV}/c^2$ for angles χ , θ_ω , α_K and β_ω defined in the text; histograms show the fit and the lower shaded histograms the background, taken from sidebands. The dashed histograms show the acceptance.

Fig. 4 shows distributions for four angles after selecting $M_{KK} > 2000 \text{ MeV}/c^2$. The angle χ is the angle between the decay plane of $\omega \rightarrow \pi^+\pi^-\pi^0$ and the decay plane $X \rightarrow K\bar{K}$; θ_ω is the production angle of the ω in the J/ψ rest

frame. The angle α_K is the decay angle of the K in the rest frame of X , taken with respect to the direction of the recoil ω ; β_ω is the angle between the normal to the ω decay plane and the beam direction. The distribution for $\cos\alpha_K$ is distinctly non-isotropic, although after integrating over all but one of the angles, much of the spin information is lost; the full amplitude analysis is much more reliable than projections on to individual angles. The dashed curves illustrate the acceptance. The shaded histograms at the bottom of each panel show background, which is taken from sidebins.

A marginal improvement of 21 in log likelihood may be obtained by adding $f_0(2100) \rightarrow K^+K^-$. However, this is not sufficient to be sure of its presence, so it is omitted.

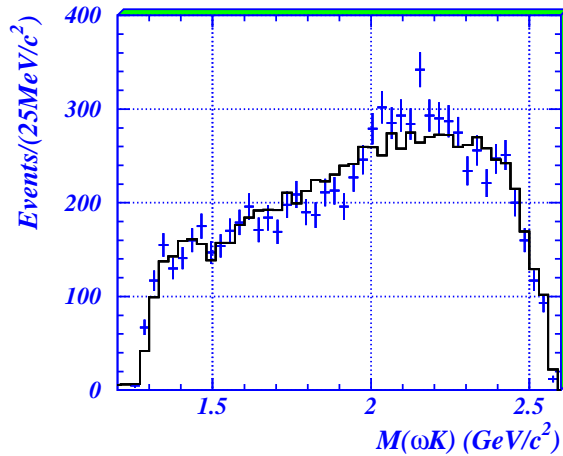


Fig. 5. The projection on to $M(\omega K^\pm)$ omitting the ωK signal at 1945 MeV/ c^2 .

The ωK mass distribution is fitted poorly unless a component decaying to ωK is included with $M \sim 1945$ MeV/ c^2 , $\Gamma \sim 270$ MeV/ c^2 . Fig. 5 shows the poor fit without this additional amplitude; no background appears capable of explaining this effect. The optimum fit is obtained with orbital angular momentum $\ell = 0$ in the ωK system, i.e. $J^P = 1^+$; this improves log likelihood by 113, and contributes 9.4% of all events. The observed isotropic decay can be fitted not only by $J^P = 1^+$, but through conspiracy between several production amplitudes for $J^P = 2^-$ and 0^- . The known $K_2(1820)$ with $J^P = 2^-$ and $K(1830)$ with $J^P = 0^-$ [9] do not alone give an adequate fit but may make some contribution. Our conclusion is that some ωK contribution is needed in this mass range, but cannot be identified cleanly and could be a superposition of more than one resonance with $J^P = 1^+$, 0^- and 2^- . Conclusions about f_0 and f_2 components are insensitive to this ambiguity. At lower masses, inclusion of $K_1(1400) \rightarrow \omega K$ also gives a significant improvement of 81 in log likelihood.

In summary, the main features of the data are peaks which may be attributed to $f_0(1710)$, $f_2(2150)$, $f_2(1270)$ and either $f_2'(1525)$ or $f_2(1565)$. An upper limit of 0.11 is set on the ratio $BR[f_0(1710) \rightarrow \pi\pi]/BR[f_0(1710) \rightarrow K\bar{K}]$. This

upper limit could rise to 0.16 if there is a fortuitous cancellation of $f_0(1710)$ and $f_0(1770)$ in $\omega\pi\pi$ data in both magnitude and phase.

The BES collaboration thanks the staff of BEPC for their hard efforts. This work is supported in part by the National Natural Science Foundation of China under contracts Nos. 19991480,10225524,10225525, the Chinese Academy of Sciences under contract No. KJ 95T-03, the 100 Talents Program of CAS under Contract Nos. U-11, U-24, U-25, and the Knowledge Innovation Project of CAS under Contract Nos. U-602, U-34(IHEP); by the National Natural Science Foundation of China under Contract No.10175060(USTC), No.10225522 (Tsinghua University); and the U.S. Department of Energy under Contract No.DE-FG03-94ER40833 (U Hawaii). We wish to acknowledge financial support from the Royal Society for collaboration between the BES group and Queen Mary, London.

References

- [1] J.Z. Bai *et al.*, (BES Collaboration), *The σ Pole in $J/\psi \rightarrow \omega\pi^+\pi^-$* , Phys. Lett. B (to be published) and hep-ex/0406038.
- [2] G.J. Feldman *et al.*, Phys. Rev. Lett. **33C**, 285 (1977).
- [3] A. Falvard *et al.*, Phys. Rev. **D38**, 2706 (1988).
- [4] L. Köpke and N. Wermes, Phys. Rep. **174**, 67 (1989).
- [5] J.Z. Bai *et al.*, (BES Collaboration), Nucl. Instr. Meth. **A458**, 627 (2001).
- [6] B.S. Zou and D.V. Bugg, Euro. Phys. J **A16**, 537 (2003).
- [7] J.Z. Bai *et al.*, (BES Collaboration), *Study of $J/\psi \rightarrow \phi\pi^+\pi^-$ and ϕK^+K^-* , to be submitted to Phys. Lett. B.
- [8] J.Z. Bai *et al.*, (BES Collaboration), Phys. Rev. **D68**, 052003 (2003).
- [9] S. Eidelman *et al.*, (Particle Data Group), Phys. Lett. **B592**, 1 (2004).